journal

J. Am. Ceram. Soc., 85 [6] 1553–60 (2002)

Failure of Crossply Ceramic-Matrix Composites

Michael P. O'Day and William A. Curtin

Division of Engineering, Brown University, Providence, Rhode Island 02912

The fast-fracture and stress-rupture of a crossply ceramic-matrix composite with a matrix through-crack are examined numerically to assess the importance of fiber architecture and the associated stress concentrations at the 0/90 ply interface on failure. Fiber bridging in the cracked 0 ply is modeled using a line-spring bridging model that incorporates stochastic and time-dependent fiber fracture. A finite-element model is used to determine the stresses throughout the crossply in the presence of the bridged crack. For both SiC/SiC and a typical oxide/oxide, the fast-fracture simulations show that as global failure is approached, a significant fraction of fibers near the 0/90 interface are broken, greatly reducing the stress concentration. For fibers with low Weibull moduli (m < 10), the tensile strength is thus nearly identical to that of a unidirectional composite scaled by the appropriate fiber volume fraction, while for fibers with larger Weibull moduli (m ≥ 10), there are modest (10−17%) reductions in tensile strength. Stress-rupture simulations show that initially high stress concentrations are relieved as fibers fail with evolving time near the 0/90 interface and shed load away from the interface. For a wide range of fiber properties, efficient load redistribution occurs such that the crossply rupture lifetime is generally within an order of magnitude of the unidirectional lifetime, when the applied stress is normalized by the relevant fast-fracture strength. Overall, stress concentrations at the 0/90 interface are largely relieved with increasing load or time due to the nonlinear bridging response and preferential fiber failure near the interface, resulting in crossplies that respond very similarly to unidirectional composites.

I. Introduction

The behavior of unidirectional ceramic-matrix composites (CMCs) loaded in tension has been well established experimentally and can be accurately predicted by existing models.[1,2] However, because of their anisotropy, both in modulus and strength, unidirectional composites are unsuitable for many applications. This has led to the predominant use of crossply and woven composites. The analytical results for unidirectional composites that relate constitutive fiber, matrix, and interface properties to the stress–strain behavior and ultimate tensile strength (UTS) do not apply directly to crossply systems. Analytic models for fiber bridging, which play an important role in crossplies, are also not generally applicable because the typical analyses (e.g., Marshall, Cox, and Evans,[3] Danchaivijit and Shetty,[4] and McCartney[5]) are only strictly valid for elastically homogeneous materials. Thus, new methods of analysis are needed.

The first damage mode in most crossply CMCs is matrix cracking. Matrix cracks typically start in the 90 plies and propagate through the 0 plies, leading to through-thickness matrix cracks that are bridged by fibers in the 0 plies, as shown in Fig. 1(a). Bridging only in the 0 plies leads to stress concentrations in the bridging fibers near the 0/90 interface and failure of the composite is ultimately caused by the failure of the bridging fibers. The stresses in the bridging fibers of a crossply material have been determined by Xia *et al.*[6] for elastically homogeneous materials, while earlier work focused on partially bridged cracks in unidirectional materials.[7] All of these works used the classic line-spring model and the bridging law of Marshall, Cox, and Evans,[3] but with no fiber failure. Stress concentrations alone are also not sufficient for predicting failure; i.e., the tensile strength is not the unidirectional strength divided by the maximum local stress concentration. Damage, i.e., fracture of some fraction of the bridging fibers, lessens the stress concentrations. The coupled phenomena of stress concentrations and fiber damage, and their influence on damage and strength in crossplies, that pervade the mechanics of composites with complex fiber architectures have not yet been studied.

The majority of the literature has simply neglected the fiber architecture, the possible stress concentrations, and the local fiber damage and proceeded to predict the tensile strength as if the material were a unidirectional composite. In other words, if the strength of a unidirectional composite of fiber volume fraction f is σ_{uts}^{uni}, then the tensile strength of a crossply or woven system of the same material has been estimated simply as $(f_1/f)\sigma_{uts}^{uni}$, where f_1 is the fiber volume fraction in the direction of loading; typically $f_1 = f/2$. This result has proven accurate in the prediction of strength in a number of different CMC systems.[8,9] One major reason for the success of the simple model is that, at the failure stress, there is typically a very high density of matrix cracks and, according to the results of Xia *et al.*,[6] the stress concentrations become small in most cases. Not all composite systems have high crack densities near failure, however. Some systems also have high fiber/matrix interfacial shear stresses, which cause higher stress concentrations. The important system of SiC/SiC can have both low crack densities and high interfacial shear stresses. In fact, such conditions tend to be optimal for design: low crack densities are usually coincident with high proportional limits so that materials can operate at reasonably high stresses with little or no damage, while high interfacial shear stresses lead to higher composite strengths.

Under typical application situations of moderate stresses (well below the ultimate tensile strength), CMCs with matrix cracks must also survive at high temperatures for long times. In this case, time-dependent fiber fracture occurs via slow crack growth of existing flaws or other processes that can be highly stress-dependent. The reduction in stress-rupture lifetime of crossplies relative to unidirectional composites, due to architecture-induced stress concentrations and accelerated fiber damage, has not yet been studied.

In this paper, we develop a coupled microscale/macroscale numerical model to examine both fast-fracture and stress-rupture in crossply CMCs. A finite-element (FE) model is used to determine the macroscale stress distributions in the presence of a matrix through-crack bridged by fibers in the 0 plies. Stochastic quasi-static and/or time-dependent fracture of the bridging fibers is then calculated based on the stresses obtained from the FE model, and this microscale damage reduces the efficacy of the bridging and leads to stress redistribution at the macroscale. Ultimately, the accumulated fiber damage near the 0/90 interface becomes large

D. B. Marshall—contributing editor

Manuscript No. 187612. Received July 2, 2001; approved April 1, 2002.
This work was supported by NASA Glenn Research Center through Grant No. NAG3-2100 and by the AFOSR through Grant No. F49620-99-1-0027, from the Mechanics of Composite Materials program.

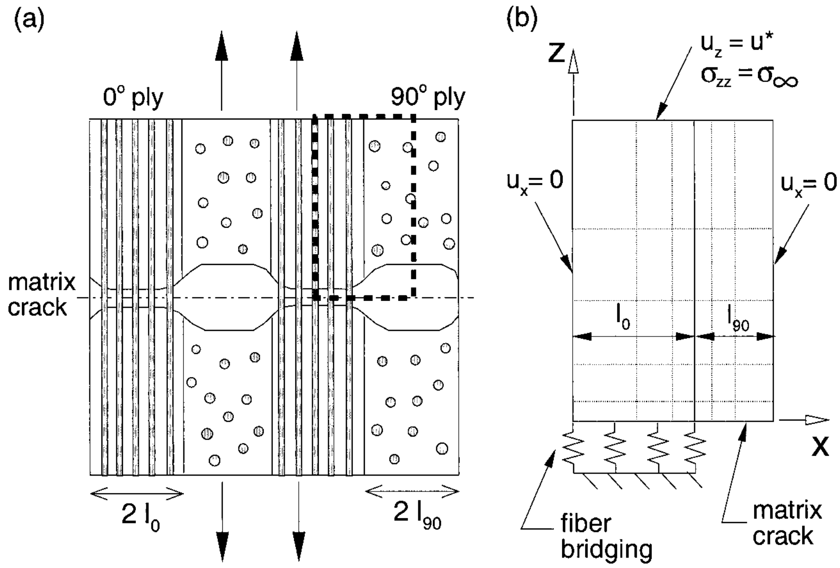

Fig. 1. (a) Representative section of periodic crossply composite, showing matrix crack and bridging in 0 plies; a unit cell is indicated by the dashed lines. (b) FE discretization of the unit cell, with boundary conditions and undeformed geometry shown.

enough to cause unstable propagation of fiber fracture across the 0 ply, corresponding to global composite failure. We compare the calculated fast-fracture strength to that estimated by the simple models based on the unidirectional strength, and find generally good agreement. This agreement stems from the fact that the softening of the bridging due to fiber damage occurs preferentially at the 0/90 boundary where the stress concentrations are high, leading to stress redistribution and a reduction in stress concentrations. The stress-rupture lifetimes of crossplies are compared with analytical and numerical determinations of unidirectional lifetimes and, at the same *normalized* applied stress, there is agreement within an order of magnitude for a wide range of fiber parameters. The preferential and accelerated damage due to high stresses at the 0/90 interface again acts to lessen the stress concentrations and deter global failure. We conclude that, in all cases, fiber damage largely relieves stress concentrations, resulting in crossplies that behave similarly to unidirectional composites.

The remainder of this paper is organized as follows. In Section II, the FE model, the fiber bridging model, and the fiber damage evolution models are all presented, and the coupling between them is described. In Section III, we present fast-fracture and stress-rupture results for SiC/SiC and oxide/oxide crossply composites, and compare their behavior to unidirectional composites. In Section IV, we provide some further discussion and conclusions.

II. Model for Unidirectional and Crossply Composites

We consider both unidirectional and 0/90 crossply composites containing a matrix crack that extends completely through all matrix material perpendicular to the fiber axis. The crack is assumed to pass around all fibers in the 0 ply, leaving them intact, as shown in Fig. 1(a). Debonding along the fiber/matrix interface is assumed to occur, with a residual interfacial sliding resistance τ acting across the debonded interface region. The composites are assumed to contain a single matrix crack; the limitations of this assumption will be discussed in Section IV. During loading, the intact fibers bridging the crack in the 0 plies will exert closure tractions on the crack surface.

(1) Fracture of Unidirectional Composites

In the unidirectional composite all fibers are parallel to the direction of applied loading. A general expression for mechanical equilibrium at the matrix crack plane has been derived by Curtin, Ahn, and Takeda.[2] Under a far-field uniaxial applied stress σ_∞ equilibrium leads to the relationship

$$\frac{\sigma_\infty}{f} = \left[1 - q(T,t)\left(1 + \frac{2l_s(x,t)}{\bar{z}}\right)\right]T(x,t) + q(T,t)\left(\frac{2l_s(x,t)}{\bar{z}}\right)\left(\frac{T(x,t)}{2}\right) \tag{1}$$

where f is the fiber volume fraction, $T(x,t)$ is the local stress carried in the unbroken fibers at time t, $q(T,t)$ is the local fraction or probability of fiber failure at the fiber stress $T(x,t)$, τ is the interfacial shear stress at the debonded/sliding fiber/matrix interface, r is the fiber radius, $l_s(x,t) = T(x,t)r/2\tau$ is the fiber slip length determined from a shear-lag model, and $\bar{z}$ is the average matrix crack spacing. Although the unidirectional composite has translational invariance in x, $T(x,t)$ is written in anticipation of the crossply system, where stress (and thus the fiber damage parameter $q(T,t)$) may vary in x as well as in time t. Here, Eq. (1) is simplified by taking $\bar{z} \to \infty$ to model a single matrix crack leading to

$$\frac{\sigma_\infty}{f} = [1-q(T,t)]T(x,t) \tag{2}$$

(A) Fast-Fracture: In fast-fracture, the time-independent fiber damage $q(T)$ arises from existing flaws in the fiber. Specifically, a two-parameter Weibull model gives the probability of failure in a length dz of fiber, over a stress increment σ to $\sigma + \mathrm{d}\sigma$ as

$$P_f(\sigma,\mathrm{d}\sigma,\mathrm{d}z) = \frac{m\sigma^{m-1}}{L_0\sigma_0^m}\,\mathrm{d}z\,\mathrm{d}\sigma \tag{3}$$

where σ_0 is the characteristic fiber strength at a gauge length of L_0 and m is the Weibull modulus. A critical fiber strength σ_c and critical gauge length $\delta_c = r\sigma_c/\tau$ can be identified for the problem, with

$$\sigma_c = \left(\frac{\sigma_0^m \tau L_0}{r}\right)^{1/(m+1)} \tag{4}$$

where we expect to find one flaw of strength σ_c in a length δ_c of fiber. In the shear-lag fiber stress field around the matrix crack (maximum at the crack plane, and decreasing linearly until the far-field stress is attained), the probability of fiber failure is[10]

$$q(\tilde{T}) = 1 - \exp\{[-1/(m+1)]\tilde{T}(x)^{m+1}(1+m\alpha^{m+1})\} \tag{5}$$

where $\alpha = fE_f/E_c$, with E_f and E_c the fiber and overall composite Young's moduli, respectively, and a tilde denotes a stress quantity normalized by σ_c. Using Eq. (2) the applied stress σ_∞ can be related to the fiber stress $T(x)$ by

$$\tilde{\sigma}_\infty = f\tilde{T}(x)\exp\{[-1/(m+1)]\tilde{T}(x)^{m+1}(1+m\alpha^{m+1})\} \tag{6}$$

Failure is the point at which no further increase in applied stress is possible with increasing fiber stress $T(x)$, or

$$\frac{d\tilde{\sigma}_\infty}{d\tilde{T}} = 0 \tag{7}$$

so that the UTS of the unidirectional composite with a single matrix crack is

$$\tilde{\sigma}_{uts}^{uni} = f\left[\frac{1}{1+m\alpha^{m+1}}\right]^{1/(m+1)} e^{-1/(m+1)} \tag{8}$$

To apply the unidirectional result (8) to a crossply composite, a scaling factor based on relative ply widths must be introduced. At the matrix crack in a crossply composite, only the 0 plies carry load. Thus, for a crossply composite having respective ply widths of l_0 and l_{90} the crossply tensile strength can be estimated as

$$\sigma_{uts}^{cp} = \sigma_{uts}^{uni}\left(\frac{l_0}{l_0 + l_{90}}\right) \tag{9}$$

This is the analytic result for the UTS of a crossply composite based strictly on the unidirectional theory. Effectively, this neglects any contribution of stress concentrations in driving crossply failure. In Section III(1), the predicted crossply tensile strength from Eq. (9) will be compared with the FE results.

(B) Stress-Rupture: Under stress-rupture conditions, the composite is subjected to a constant far-field stress while time evolves, resulting in increasing fiber damage due to degradation of the fibers. Eventually, the composite will have damaged enough that the overall load level can no longer be maintained. The point at which damage propagates unstably across the composite is the stress-rupture lifetime at the given tensile stress. In this case, Eq. (2) still holds, but the damage parameter $q(T,t)$ becomes time-dependent.

Here we assume that fiber degradation in time is governed by slow crack growth of existing flaws in the fiber. A Paris law describes the rate of crack growth as

$$\frac{da}{dt} = AK^\beta \tag{10}$$

where a is the current crack length, K is the crack tip stress intensity factor, and β and A are the (possibly temperature-dependent) crack growth exponent and rate constant, respectively. The stress intensity factor for tensile loading of a fiber is

$$K = \sigma_f(z,t)Y\sqrt{a} \tag{11}$$

where Y is a geometric factor, and the fiber stress $\sigma_f(z,t)$ is a function of both position z along the length of the fiber relative to the matrix crack at $z = 0$ and time. The critical Mode I stress intensity factor defines the strength S of a flaw of length a as

$$K_{Ic} = SY\sqrt{a} \tag{12}$$

Substitution of Eq. (11) into Eq. (10) and integrating yields an evolution equation for the flaw length. Using Eq. (12) the evolution of flaw strength $S(z,t)$ is

$$\tilde{S}(z,\tilde{t}) = [\tilde{S}_i(z)^{\beta-2} - \int_0^{\tilde{t}} \tilde{\sigma}_f(z,\tilde{t}')^\beta \, d\tilde{t}']^{1/(\beta-2)} \tag{13}$$

where the initial flaw strength is $S_i(z)$ and the following normalizations have been introduced:

$$\tilde{t} = tC\sigma_c^2 \tag{14a}$$

$$C = \left(\frac{\beta}{2} - 1\right) AY^2 K_{Ic}^{\beta-2} \tag{14b}$$

The probability of failure in length dz of fiber, over the stress increment σ to $\sigma + d\sigma$ is identical to Eq. (3), with the stress σ replaced by the initial flaw strength $S_i(z)$, thus

$$P_f(\sigma, d\sigma, dz) = \frac{mS_i^{m-1}}{L_0\sigma_0^m}\, dz\, dS_i \tag{15}$$

We simplify the fiber stress profile by neglecting any failure in the far-field. According to the shear-lag fiber stress profile, the fiber stress decreases linearly with distance away from the matrix crack until the far-field fiber stress level is reached. The fiber slip length $l_s(t) = T(t)r/2\tau$ is the distance over which the fiber stress would decrease to zero were it not interrupted by the far-field fiber stress. The simplified fiber stress profile is

$$\sigma_f(z,t) = T(t)\left(1 - \frac{z}{l_s(t)}\right) \qquad (\text{for } |z| < l_s(t)) \tag{16}$$

which decreases linearly from the maximum value $T(t)$ at the matrix crack to zero at a distance l_s away from the matrix crack. The evolution of this simplified fiber stress profile is shown in Fig. 2. In this stress field, the probability of fiber failure anywhere along the slip length at any time up to the current time is[10]

$$q(\tilde{T},\tilde{t}) = 1 - \exp\left\{-\frac{2}{\delta_c}\int_0^{l_s(\tilde{t})}\left[\tilde{T}(\tilde{t})^{\beta-2}\left(1 - \frac{z}{l_s(\tilde{t})}\right)^{\beta-2} + \int_o^{\tilde{t}} \tilde{T}(\tilde{t}')^\beta \left(1 - \frac{z}{l_s(\tilde{t}')}\right)^\beta d\tilde{t}'\right]^{m/(\beta-2)} dz\right\} \tag{17}$$

where $q(\tilde{T},\tilde{t})$ is now explicitly a function of time. The stress-rupture lifetime of a unidirectional composite, at some constant

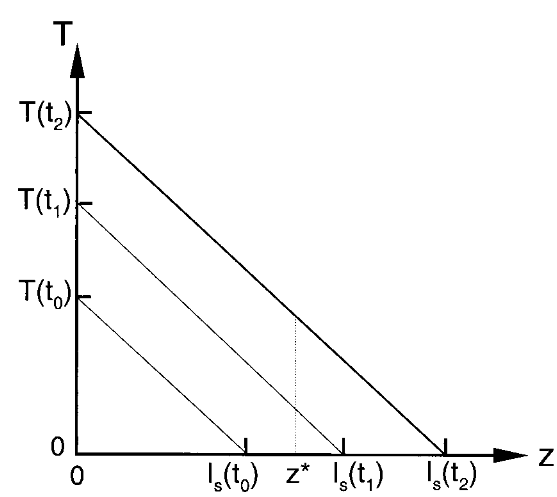

Fig. 2. Evolution of simplified shear-lag fiber stress profile with time around a matrix crack at $z = 0$.

remote stress, can then be found by solving the coupled Eqs. (17) and (2). An iterative scheme is used to obtain a self-consistent solution at a given time. Time is then incremented by some small amount, and a new solution is sought. The time at which no converged solution exists corresponds to the stress-rupture lifetime for a unidirectional composite.

(2) Finite-Element Model

The FE method is applied to simulate both fast-fracture and stress-rupture. The following discussion relates to the FE model in general; aspects unique to each simulation type will be mentioned when appropriate. In formulating the macroscale mechanics problem, a continuum approach is adopted. The discrete fibers and matrix are replaced by a homogeneous, isotropic material with effective properties for each ply. The effective Young's modulus for the 0 ply corresponds to that for uniaxial loading of a single laminate along the fiber direction (longitudinal) and for the 90 ply corresponds to the transverse Young's modulus of a single laminate. The effective properties were determined from an Eshelby analysis,[11] using the constituent properties given in Table I.

Because of the periodic nature of the 0/90 laminate, a unit cell geometry is appropriate. The unit cell and its FE discretization are shown in Figs. 1(a) and (b), respectively. The left and right edges of the unit cell correspond to the centers of the 0 and 90 plies, respectively. The left and right edges are constrained in the x direction and the z displacement of the top edge is prescribed, as discussed below. The extent of the composite in the y direction is assumed to be large enough such that plane strain conditions prevail. The model height h is taken to be $3(l_0 + l_{90})$, which ensures that far-field stress gradients in z are small. Approximately 1100 bilinear plane strain quadrilateral elements comprised the FE mesh. The mesh is weighted to concentrate nodes near the matrix crack plane and the ply interface. All relevant geometric parameters are given in Table I.

The prescribed displacement of the top edge is unique to the simulation being performed. In the fast-fracture simulation, the z displacement of the top edge is monotonically increased until composite failure occurs. In stress-rupture the goal is to maintain a constant level of remote stress, which is accomplished as follows. Over a very small time the composite is loaded to the desired remote stress level. Because of the difference in 0 and 90 ply moduli, as well as the bridging stress variation along the matrix crack, the remote stress is expected to vary in x along the top edge. The average tensile stress over the entire top edge is to be held constant at the desired level, but the FE model is loaded through prescribed displacements. In general, as damage accumulates, a greater incremental displacement is required to maintain the constant remote stress level. In the FE procedure, the current remote stress and remote stress history are used to predict the necessary incremental displacement to satisfy the constant remote stress condition. Fluctuations from the desired stress level are on the order of 0.01%.

The effect of fiber bridging at the matrix crack plane is introduced through a continuum nonlinear spring bridging law, devised by Danchaivijit and Shetty[4] (DS), which incorporates the physically correct fiber stresses in the uncracked matrix material. In the absence of any fiber damage and uniform remote loading, the DS bridging law relates the closure traction $p(u)$ to the crack opening displacement $2u(x)$ according to

$$p(u) = \frac{\eta\sigma_\infty}{2(1+\eta)}\left\{\left[1 + \frac{16(1+\eta)^2 E_f f^2 \tau u(x)}{\eta^2\sigma_\infty^2 r}\right]^{1/2} + 1\right\} \tag{18}$$

where $\eta = fE_f/(1-f)E_m$, and E_m is the matrix modulus. We include the effects of fiber failure, represented by the damage parameter q as follows. We assume that in each small region of the composite dx around point x there are a sufficient number of fibers such that the local response is identical to that of a unidirectional composite. The local fiber stress $T(x)$ induces fiber damage q which evolves according to either Eq. (5) or Eq. (17) for fast-fracture and stress-rupture simulations, respectively. $T(x)$ is obtained as a self-consistent outcome of the FE calculation. Fiber damage q due to the load $T(x)$ then acts to weaken the bridging law by reducing the fraction of fibers participating in the bridging as

$$p(u,q) = (1-q)\,p(u) \tag{19}$$

where $1 - q$ is the local probability of fiber survival. The dependence of the bridging law, $p(u,q)$, on the local damage state q is explicit, and position dependence x and time dependence, if applicable, are implicit in u and q.

An iterative solution procedure is used to obtain a self-consistent solution in displacements, fiber stresses, and fiber damage. A typical FE iteration proceeds as follows. The incremental displacement of the top edge is prescribed. For any iteration (not yet converged) within this displacement increment, the displacement field of the entire model was determined by the FE solution from the previous iteration. The stress in intact fibers at the ith node (position x_i) bridging the matrix crack is calculated directly from the nodal displacements as $T_i = p(u_i,q_i)/f(1-q_i)$, where q_i and u_i were obtained in the previous iteration. Using T_i, the probability of failure at the ith node is found from either Eq. (5) or Eq. (17), in accordance with the type of simulation being performed. The line-spring stiffness contributions at the matrix crack are then $k_i = [\mathrm{d}p(u_i,q_i)/\mathrm{d}u_i]|_{q_i}$, with $p(u,q)$ given by Eqs. (19) and (18). These are assembled into the global FE equations, which are solved to provide the new displacement field. This procedure is repeated until the displacement solution converges. When the solution has converged, the next incremental displacement is applied.

In fast-fracture simulations, evaluation of fiber damage by Eq. (5) is clear. For stress-rupture Eq. (17) must be integrated numerically, as follows. At some time $\tilde{t}$ and at every position x, the bracketed term in the integrand of Eq. (17) must be integrated over the length of the fiber, up to the current slip length $l_s(\tilde{t})$. Evaluation of the first term inside the brackets is straightforward, but the nature of the time-varying slip length $l_s(t')$ in the second term requires that the lower limit of the time integral be modified. Within the present assumption of no far-field fiber stress, the slip length and stress profile evolution along any fiber is shown in Fig. 2, where $z = 0$ represents the matrix crack. When the position integral in Eq. (17) is evaluated at some z^*, the time integral is physically meaningful only at times $\tilde{t}'$ such that $z^* \le l_s(\tilde{t}')$. From Fig. 2, we see that the stress at z^* is zero until the slip length increases such that $z^* \le l_s(\tilde{t}^*)$. This means that for any time less than $\tilde{t}^*$, the point z^* does not contribute to the time integral. Computationally, the lower limit of the time integral in Eq. (17) thus becomes $\tilde{t}^*$ with no loss in generality.

Several checks were used to verify the FE model. The FE fast-fracture strengths of unidirectional composites were compared with the analytical UTS, Eq. (8), and were in exact agreement. The FE stress-rupture lifetime of a unidirectional composite was compared with the analytical lifetime, obtained by solving the coupled Eqs. (17) and (2), and again the FE results were in exact agreement.

Table I. FE Input Material and Geometric Parameters

	E_f (GPa)	ν_f	E_m (GPa)	ν_m	f	σ_c (GPa)	r (μm)	τ (MPa)	l_0 (μm)
SiC/SiC	269	0.16	310	0.16	0.342	2	7.5	97	156
Oxide/Oxide	372	0.2	124	0.2	0.248	1	6	25	122

III. Results

FE simulations were performed for a SiC/SiC composite and a typical oxide/oxide. The overall trends observed were similar for the two systems; thus we present fast-fracture results for the SiC/SiC system and stress-rupture results for the oxide/oxide.

(1) Fast-Fracture Results

The normalized continuum bridging stress $p(u,q)/\sigma_{\text{uts}}^{\text{uni}}$ and fiber damage parameter q are shown for the SiC/SiC composite in Figs. 3(a) and (b), respectively, at various levels of applied loading. At loads less than 50% of the crossply UTS, a relatively large stress concentration (approaching 2) exists but a negligible percentage of fibers have fractured. With increasing load, fiber damage accumulates more rapidly, particularly near the 0/90 interface, reducing the stress concentration. At an applied stress of ~85% of the crossply UTS, the region of the 0 ply at the 0/90 interface just reaches the limiting value of the unidirectional UTS $\sigma_{\text{uts}}^{\text{uni}}$. Since no region of the 0 ply can exceed $\sigma_{\text{uts}}^{\text{uni}}$, as the applied stress is increased the near-interface region sheds load to fibers away from the interface. Simultaneously, with increasing strain, fibers in the near-interface region are damaging so rapidly that this region actually supports a decreasing amount of stress. Figure 3(a) shows that, at failure, the stress in the highly damaged near-interface region is significantly below the unidirectional failure stress. The evolving damage softens the near-interface region significantly and decreases the stress concentration as the applied stress is increased further. The net result is an almost complete elimination of the stress concentration, and hence the tensile strength is well approximated by the scaled unidirectional theory, as discussed further below.

It is useful to examine the local bridging law at several locations along the 0 ply. The DS bridging law, Eq. (18), describes $p(u)$ as a monotonic function of u, but the bridging is not monotonic when fiber damage occurs. With damage, the bridging law has hardening ($\mathrm{d}p(u)/\mathrm{d}u > 0$) and softening ($\mathrm{d}p(u)/\mathrm{d}u < 0$) regimes. Figure 4 shows the bridging history of four points along the 0 ply, up to composite failure. As implied by the failure stress distribution of Fig. 3(a), the most heavily damaged regions evolve on the softening portion of the bridging law. Globally, the composite is stable even though local regions of softening exist. Figure 4 also shows that all points of the 0 ply basically follow the same underlying bridging law; it is the degree of local stress concentration and fiber damage that determines how much bridging actually occurs. The slightly different bridging described in Fig. 4 is solely due to the σ_∞ dependence of the DS bridging law. Indeed for an MCE-type law with $p(u) = Au^{1/2}$, where A is a constant independent of remote stress, the curves in Figure 4 collapse to a single curve and the bridging law of Eq. (19) is unique.

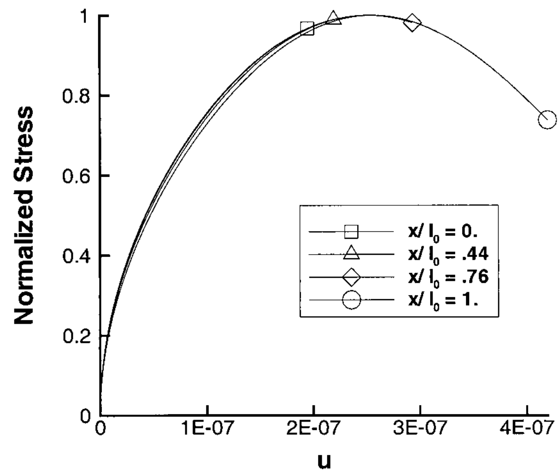

Fig. 4. Bridging law history at four points along the 0 ply (SiC/SiC, $m = 5$); symbol denotes global crossply failure and stress is normalized by $\sigma_{\text{uts}}^{\text{uni}}$.

The FE determination of the UTS is compared with the simple analytical prediction, Eq. (9), for both composite systems in Table II. We have considered a balanced crossply ($l_{90} = l_0$) and $l_{90} = 2L_0$, which can roughly approximate current woven materials with the longitudinal tows represented by the 0 ply and the transverse tows and matrix-rich regions roughly represented by the wider 90 ply. At lower Weibull moduli ($m = 5$) the scaled unidirectional theory slightly overpredicts the UTS of the crossply SiC/SiC system. For larger values of Weibull modulus ($m = 20$), the crossply UTS is significantly below the analytic theory. The oxide/oxide system (not shown) shows slightly smaller stress concentrations and greater ability to relieve them by damage. Thus, the oxide/oxide UTS follows the trends found for SiC/SiC but the differences with the scaled unidirectional prediction are even smaller.

The variation of the Weibull modulus was performed at a fixed value of σ_c (see Table I). As the Weibull modulus increases, the stress range over which fiber damage occurs narrows. In the limiting case of an infinite Weibull modulus, failure becomes extremely brittle and occurs at the instant any point along the 0 ply

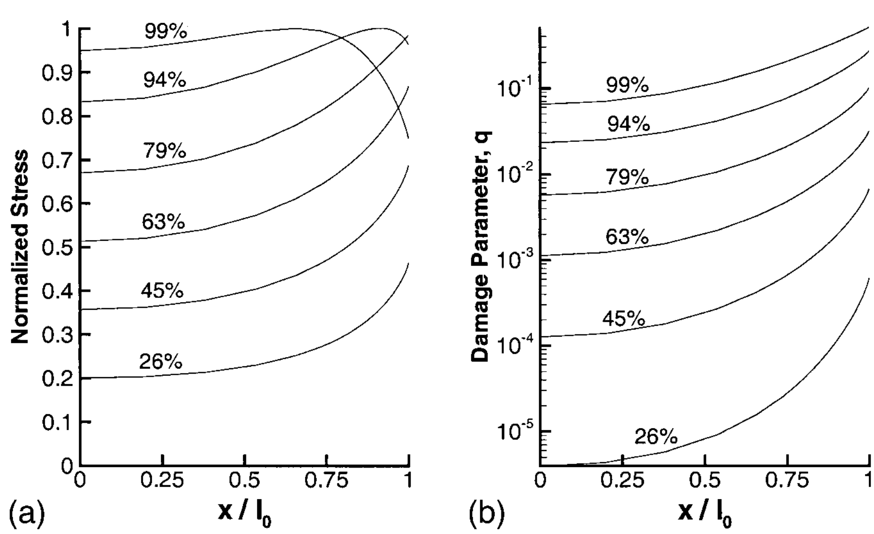

Fig. 3. Fast-fracture behavior for balanced ($l_0 = l_{90}$) SiC/SiC composite, $m = 5$: (a) normalized bridging stress versus distance along 0 ply; (b) fiber damage parameter versus distance along 0 ply matrix crack. Quantities are shown at various percentages of the applied stress to eventual crossply UTS.

Table II. Comparison of FE and Analytical Fast-Fracture UTS (MPa)

		SiC/SiC			Oxide/oxide		
		$m = 5$	$m = 10$	$m = 20$	$m = 5$	$m = 10$	$m = 20$
$l_{90} = l_0$	Eq. (9)	289	313	326	104	113	118
	FEM	277	284	278	101	106	104
$l_{90} = 2l_0$	Eq. (9)	193	208	217	69	75	79
	FEM	183	186	181	66	69	68

reaches the unidirectional tensile strength and hence stress concentrations play a major role. Damage tolerance in the fiber bundle (lower *m*) is thus one key element for reduction of local stress concentrations.

The bridging stress along the matrix crack at incipient failure, normalized by σ_{uts}^{uni}, is shown in Fig. 5 for a range of Weibull moduli. An increasing Weibull modulus results in less stress redistribution to fibers away from the interface and thus larger remaining stress concentrations. Therefore, with an increasing Weibull modulus the scaled unidirectional theory will increasingly overpredict the actual crossply UTS, as seen in Table II.

(2) Stress-Rupture Results

The main result of the stress-rupture analysis is Fig. 6, which compares the stress-rupture lives of unidirectional and crossply (oxide/oxide) composites at various remote stress levels, normalized by the respective fast-fracture strengths. This normalization permits a direct comparison of crossply and unidirectional composites. Increasing β values are shown to increase the difference between unidirectional and crossply lives at a given load level. Only when β becomes large and the stress level is less than half of the fast-fracture strength does the difference in lifetimes of unidirectional and crossply composites approach an order of magnitude.

The time evolution of the bridging stress depends on the ratio of remote stress to fast-fracture strength of the crossply. At high ratios ($\geq$90%) of the fast-fracture strength, significant fiber fracture occurs just in loading up the composite. Thus the stress concentration is partially relieved before any time-dependent damage begins to accumulate, and time-dependent effects are minor. Time-dependent effects are more prominent at lower ratios of applied stress to UTS ($\sim$50%), where initial stress concentrations are larger due to less stress-driven damage. The bridging stress and damage at various time increments are shown in Fig. 7, with $m = 5$ and $\beta = 5$, when the applied stress is 50% of the crossply fast-fracture strength. Initially, with evolving time, the

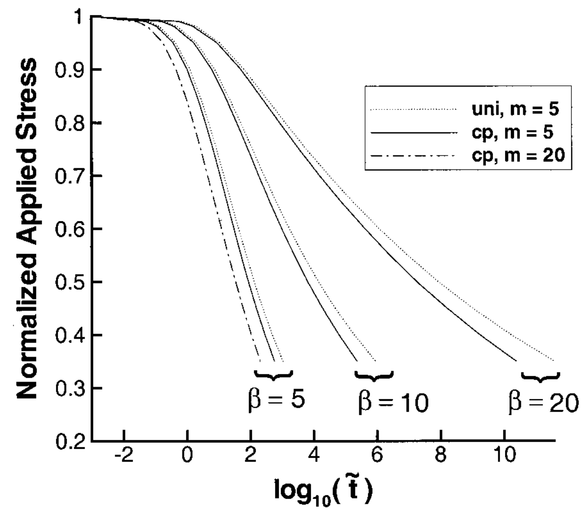

Fig. 6. Oxide/oxide composite lifetimes at various normalized applied stress levels $\sigma_\infty/\sigma_{uts}$.

near-interface region softens, reducing the stress concentration. Damage increases rapidly in this area, resulting in load shedding away from the interface, and continued softening near the interface. Eventually, the near-interface region has no intact fibers ($q = 0$), but since the applied stress is fairly low the composite is still globally stable. Ultimately, this region of complete fiber failure propagates into $\sim$10% of the 0 ply just before failure. At this point, the location of the maximum bridging stress actually is located in the center of the 0 ply.

The role of fiber Weibull modulus in the stress-rupture behavior of crossplies was also examined. In the fast-fracture simulations, lower values of Weibull modulus were shown to contribute to efficient load shedding away from the 0/90 interface. Figure 8 shows the bridging traction and damage at various times at 50% of the fast-fracture strength, for $m = 20$ and $\beta = 5$. As compared with the $m = 5$ system, the stress concentration is relieved to a lesser extent. Damage near the 0/90 interface tends to accumulate faster and the composite is unable to shed load away from the interface, leaving the center of the zero ply with relatively little damage and low stress. Immediately before failure, a stress concentration is still present, and complete fiber failure has propagated into $\sim$30% of the 0 ply. With all other parameters unchanged, the composite with $m = 20$ fails an order of magnitude faster than the $m = 5$ composite. Lifetimes of the $m = 5$ and $m = 20$ composites over the full applied stress range are shown in Fig. 6. Similar to the fast-fracture observations, a lower Weibull modulus again promotes stress redistribution, resulting in crossplies that behave similarly to unidirectional composites.

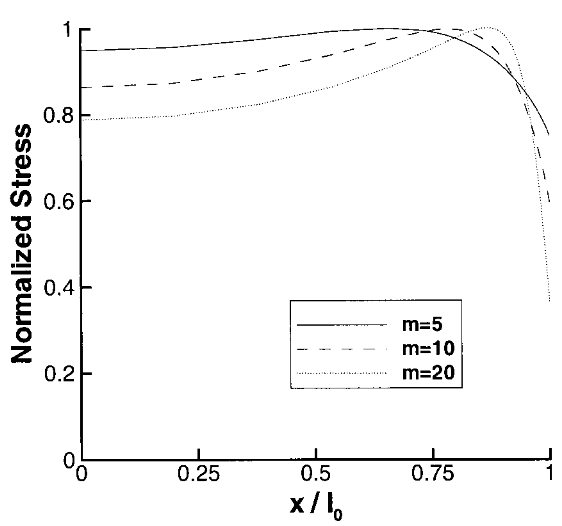

Fig. 5. Normalized stress distribution of 0 ply at failure for various Weibull moduli (SiC/SiC composite).

IV. Summary and Discussion

The fast-fracture and stress-rupture of crossply composites, and the effects of local stress concentrations, have been modeled numerically. In fast-fracture, interface stress concentrations do induce local fiber damage but these, in turn, reduce the stress concentrations at higher applied loads. The fiber Weibull modulus

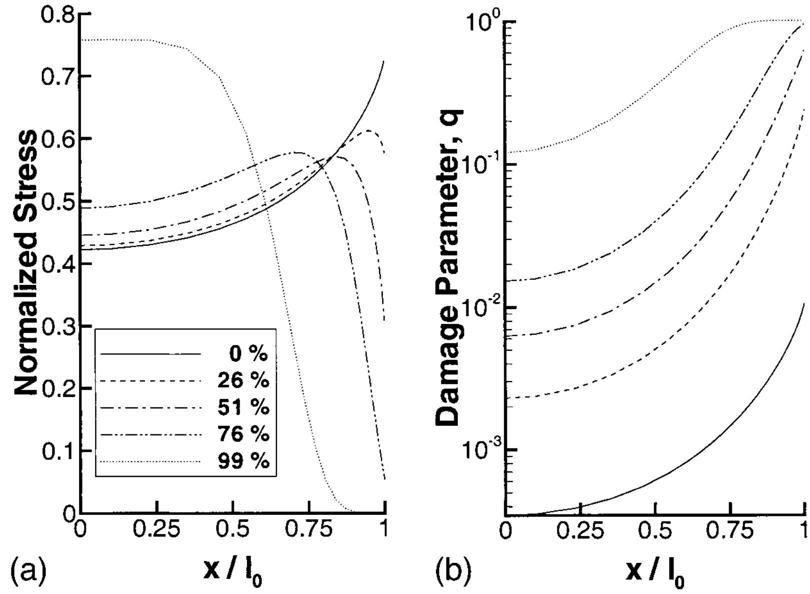

Fig. 7. Rupture behavior for a balanced ($l_0 = l_{90}$) oxide/oxide composite with low m (=5) and low β (=5) at remote stress of 50% of fast-fracture UTS: (a) normalized bridging stress versus distance along 0 ply; (b) fiber damage parameter q vs distance along 0 ply; shown at various percentages of the stress-rupture lifetime.

is shown to be the key parameter to obtain efficient load shedding away from the highly damaged near-interface region. A low Weibull modulus promotes stress redistribution and tensile failure occurs at stresses only slightly less than those predicted by the analytic theory, thus validating the general accuracy of the analytic predictions. As the fiber Weibull modulus increases, the analytic theory tends to overpredict the composite UTS. In addition, while Eq. (8) predicts monotonically increasing UTS with increasing Weibull modulus for unidirectional composites, the numerical results suggest that, for the systems studied here, the crossply UTS is relatively insensitive to changes in m, as shown in Table II. The stress-rupture lifetime of crossplies is generally within an order of magnitude of the corresponding unidirectional composite, for the same normalized remote load level. Crossply lifetime is seen to decrease with increasing Weibull modulus.

This work has been limited to a composite containing a single matrix crack. For most composites loaded to failure, arrays of parallel matrix cracks will form and saturate at some average spacing.[12] Thus a direct numerical comparison of the FE fast-fracture strengths to actual crossply fast-fracture strengths is not recommended. Also, if the average matrix crack spacing becomes less than half of the slip length l_s, then fiber damage can no longer be calculated in the manner described above; the effect of fiber breaks at neighboring matrix cracks will have to be considered within the framework of Curtin, Ahn, and Takeda.[2] The present FE results will tend to overpredict the crossply UTS, but the trends in comparing crossply and unidirectional behavior will be similar to those found here. The single-matrix-crack assumption becomes more appropriate in stress-rupture situations. Experiments show that a typical unidirectional oxide/oxide composite loaded to less

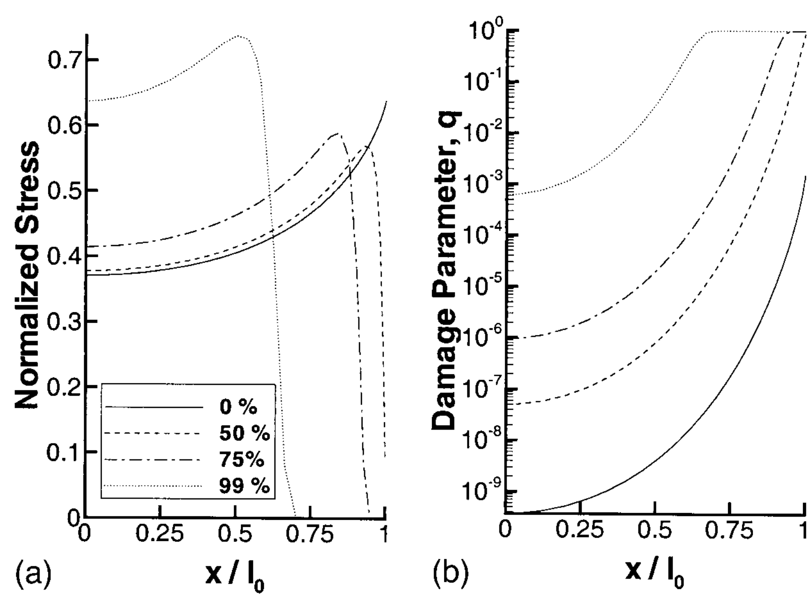

Fig. 8. Rupture behavior for balanced ($l_0 = l_{90}$) oxide/oxide composite with high m (=20) and low β (=5) at remote stress of 50% of fast-fracture UTS: (a) normalized bridging stress versus distance along 0 ply; (b) fiber damage parameter q vs distance along 0 ply; shown at various percentages of the stress-rupture lifetime.

than half of its UTS will contain less than 20% of the cracks present at the fast-fracture point.[13] Thus the average matrix crack spacing for stress-rupture (at 50% of the fast-fracture strength) is ~5 times larger than the spacing at the fast-fracture point and the single-matrix-crack assumption is justifiable for the stress-rupture simulations at such low stresses.

The present results use the line-spring bridging model. Xia *et al.*[6] critically examined the line-spring model in applications to problems of the type studied here. They concluded that in systems with significant fiber/matrix interface slip, the line-spring model overpredicts stress concentrations. A large-scale sliding (LSS) model based on an FE model was proposed to correct this deficiency. The stress concentrations in the LSS model were found to be reduced with increasing stress, decreasing fiber/matrix interfacial shear stress τ, and decreasing matrix crack spacing $\bar{z}$. We have used the line-spring model for materials where the LSS model is expected to be more appropriate. However, we have shown that as failure is approached, the interface stress concentration is largely eliminated; hence use of the line-spring model is not a serious limitation. In general, use of the line-spring model should predict a lower bound for the tensile strength. It is insightful to reexamine the fundamental continuum approximation used in bridging models, particularly the replacement of discrete fiber stresses by a smooth distributed traction. This approximation assumes that the stress concentration exists over many fibers along the matrix crack. For the SiC/SiC system studied here, assuming a rectangular fiber array, approximately seven fibers span the ply half-width l_0 . The stress concentration exists over ~40% of the model width (see Fig. 3), or only three fibers. Thus, the continuum approximation may not be extremely accurate for thin-ply materials; a model that incorporates discrete fiber bridging effects may be more appropriate.

Fiber damage represents one process by which composites can reduce stress concentrations. Mackin *et al.*[14] and others have shown that localized multiple matrix cracking itself is an effective mechanism in this role. Multiple matrix cracking that occurs preferentially around a notch or hole due to the high elastic stress concentrations is found to greatly relieve those large-scale stress concentrations. Model calculations by Genin and Hutchinson demonstrate how the loss of stiffness on cracking reduces the local stress.[15] The present work shows that the additional stress concentrations on the fibers caused by those matrix cracks, due to 0/90 ply boundaries or free edges at the notch root or hole edge, should then be greatly reduced by the stochastic fiber damage. Thus, the notched composite strength can be accurately estimated using a unidirectional strength value reduced by the net-section area fraction.

Acknowledgments

W. A. Curtin thanks Dr. H. Halverson and Dr. G. Morscher for useful discussions pertaining to this work.

References

[1]W. A. Curtin, "Theory of Mechanical Properties of Cermaic-Matrix Composites," *J. Am. Ceram. Soc.*, **74**, 2837–45 (1991).

[2]W. A. Curtin, B. K. Ahn, and N. Takeda, "Modeling Brittle and Tough Stress–Strain Behavior in Unidirectional Ceramic Matrix Composites," *Acta Mater.*, **46**, 3409–20 (1998).

[3]D. B. Marshall, B. N. Cox, and A. G. Evans, "The Mechanics of Matrix Cracking in Brittle-Matrix Fiber Composites," *Acta Metall.*, **33**, 2013–21 (1985).

[4]S. Danchaivijit and D. K. Shetty, "Matrix Cracking in Ceramic-Matrix Composites," *J. Am. Ceram. Soc.*, **76**, 2497–504 (1993).

[5]L. N. McCartney, "Mechanics of Matrix Cracking in Brittle-Matrix Fibre-Reinforced Composites," *Proc. R. Soc. London, Ser. A*, **409**, 329–50 (1987).

[6]Z. C. Xia, J. W. Hutchinson, A. G. Evans, and B. Budiansky, "On Large Scale Sliding in Fiber-Reinforced Composites," *J. Mech. Phys. Solids*, **42**, 1139–58 (1994).

[7]D. B. Marshall and B. N. Cox, "Tensile Fracture of Brittle Matrix Composites: Influence of Fiber Strength," *Acta Metall.*, **35**, 2607–19 (1987).

[8]W. A. Curtin, "Stochastic Damage Evolution and Failure in Fiber-Reinforced Composites," *Adv. Appl. Mech.*, **36**, 163–253 (1999).

[9]W. A. Curtin, *Comprehensive Composite Materials*; Ch. 4.03. Edited by A. Kelly and C. Zweben. Pergamon-Elsevier Science, Kidlington, U.K., 2000.

[10]H. G. Halverson and W. A. Curtin; unpublished work.

[11]T. W. Clyne and P. J. Withers, *An Introduction to Metal Matrix Composites*. Cambridge University Press, Cambridge, U.K., 1996.

[12]P. Karandikar and T.-W. Chou, "Characterization and Modeling of Microcracking and Elastic Moduli Changes in Nicalon/CAS Composites," *Compos. Sci. Technol.*, **46**, 253–63 (1993).

[13]D. S. Beyerle, S. M. Spearing, F. W. Zok, and A. G. Evans, "Damage, Degradation, and Failure in a Unidirectional Ceramic-Matrix Composite," *J. Am. Ceram. Soc.*, **75**, 2719–25 (1992).

[14]T. J. Mackin, T. E. Purcell, M. Y. He, and A. G. Evans, "Notch Sensitivity and Stress Redistribution in Three Ceramic-Matrix Composites," *J. Am. Ceram. Soc.*, **78**, 1719–28 (1995).

[15]G. M. Genin and J. W. Hutchinson, "Composite Laminates in Plane Stress: Constitutive Modeling and Stress Redistribution Due to Matrix Cracking," *J. Am. Ceram. Soc.*, **80**, 1245–55 (1997). □